Proceedings of the 21st ICSMGE, Vienna, Austria, 14 – 19 June 2026. Pistrol, Adam & Schweiger (eds.)
Published by: ÖGG, Austrian Society for Geomechanics, Salzburg, Austria, ISBN 978-3-9503898-4-5
https://doi.org/10.53243/ICSMGE2026-200

Evaluating Hypoplasticity, ISA-Model and NorSand in Laboratory Test Predictions: Insights from a Round-Robin Benchmarking Exercise

Gertraud Medicus
University of Innsbruck, Austria, gertraud.medicus@uibk.ac.at

Merita Tafili
Ruhr-Universität Bochum, Germany

Patrick Staubach
Bauhaus-Universität Weimar, Germany

Mina Mofrad, Mehdi Pouragha, Paul Simms
Carleton University, Ottawa, Canada

David Mašín
Charles University, Prague, Czech Republic

Andy Fourie
The University of Western Australia, Perth, Australia

Riccardo Fanni
WSP Australia

David Reid
Red Earth Engineering, Australia

ABSTRACT: Calibration and validation of constitutive models often relies on standard laboratory tests under axisymmetric conditions with initial hydrostatic stress states. However, geotechnical applications often involve three-dimensional or plane-strain conditions, including anisotropic stress states and principal stress rotation. To ensure the reliability of the models, it is essential to evaluate their performance under these broader conditions as well. Our study builds on a collaborative round-robin benchmarking exercise with 13 participating groups, focusing on predictions from three models: the hypoplastic model by von Wolffersdorff (1997), the ISA model by Fuentes & Triantafyllidis (2015), and the elastoplastic NorSand model by Jefferies (1993). The models were calibrated using standard laboratory test data from sandy silt tailings and then applied in blind predictions for hollow cylinder torsional shear (HCTS) and oedometric compression tests, targeting K_0 stress states, stress rotation, Lode angle variations, and volumetric responses. Although the blind prediction tests were relatively fundamental, the range of predictions was surprisingly wide, highlighting inconsistencies in models' performance under monotonic loading paths. Results show that hypoplasticity and the ISA model performed well, especially compared to commonly used elastoplastic models such as NorSand. While other models in the round robin also showed good performance, this study specifically examines hypoplasticity and the ISA model to understand why these models reliably predicted behaviour across various loading scenarios. We examine factors contributing to model effectiveness, including simplicity, calibration demands, and adaptability to varied loading conditions. Based on our results, we advocate for (1) clear and straightforward calibration procedures based on minimum required tests dictated by the model's complexity, and (2) avoiding multiple model calibration for various initial and/or loading conditions. Our collective exercise points toward a crucial need for more rigorous model validation based not only on accuracy for conventional loading paths, but also on the model's generality under various loading conditions.

KEYWORDS: soil constitutive modelling, hypoplasticity, elastoplasticity, round robin.

1 INTRODUCTION

Constitutive models are essential in geotechnical analyses. Their predictive performance depends on a sound theoretical formulation and a consistent calibration procedure, typically based on standard laboratory tests. Many models are developed, calibrated and validated with a focus on axisymmetric conditions, while practical geotechnical problems often involve more complex conditions, such as stress rotation, and varying Lode angles. To assess model reliability under such conditions, a round-robin benchmarking exercise was conducted with blind model predictions of oedometric and hollow cylinder torsional shear tests (Reid et al., 2026). The present study analyses a subset of this round robin, focusing on three participating groups and their respective models: hypoplasticity (Group 1: Gertraud Medicus & David Mašín), ISA model (Group 2: Merita Tafili & Patrick Staubach), and NorSand (Group 11: Mina Mofrad, Mehdi Pouragha & Paul Simms). The aim is to evaluate how well the models can predict the behaviour of the investigated sandy silt tailings under different loading scenarios. We also aim to provide a broader perspective beyond comparisons with individual experiments only.

2 CONSTITUTIVE MODELS AND THEIR CALIBRATION

While the round-robin exercise (Reid et al., 2026) included 13 submissions with 6 different constitutive models, this study focuses on the predictions of three groups - using hypoplasticity, ISA model, and NorSand - to allow for a more detailed discussion within this conference contribution. All groups calibrated the models using a set of standard laboratory tests, including drained and undrained triaxial compression tests on loose and dense samples, isotropic compression tests, and bender element measurements of shear wave velocity (Reid, 2022; Reid et al., 2026). The tests were conducted on samples prepared using air-dried (AD) and moist tamping (MT) sample preparation methods.

2.1 *Sand hypoplasticity*

Hypoplasticity is a constitutive model introduced by Kolymbas (1977) that does not use standard notions of elastoplasticity, such as elastic regions, yield surfaces, or plastic potential surfaces, nor does it assume a decomposition of strain into purely elastic and purely plastic parts. In sand hypoplasticity (von Wolffersdorff, 1996), the stress rate is expressed as a tensorial function of the current stress, void ratio, and strain rate. The model incorporates concepts from Critical State Soil Mechanics, such as the critical state locus according to Matsuoka–Nakai and a stress-dependent critical state line in the void ratio e versus mean effective stress p' plane. This enables the model to capture the influence of stress level and density on strength and stiffness predictions.

Sand hypoplasticity involves eight parameters: φ_c is the critical friction angle, h_s and n control the shape of the limiting void ratio curves (as normal compression line and critical state line). The reference void ratios e_{d0}, e_{c0} and e_{i0} define the locus of these curves. The parameter α governs the density dependence of the peak friction angle, and β controls the stiffness dependence on relative density. Details on the calibration procedure can be found in Herle (1997), Herle and Gudehus (1999), or Kadlíček et al. (2022). The parameters of hypoplasticity (Group 1) are summarized in Table 1.

Table 1. Parameters of sand hypoplasticity for the MT and AD prepared samples (Group 1).

φ_c (°)	h_s (kPa)	n	e_{d0}	e_{c0}	e_{i0}	α	β
35	50000	0.3	0.393	0.785	0.903	0.22	3

2.2 *Intergranular Strain Anisotropy (ISA) model*

The ISA model (Intergranular Strain Anisotropy), introduced by Fuentes and Triantafyllidis (2015), is a plasticity-based constitutive model originally developed for sand. Unlike classical elastoplastic models (e.g., Manzari & Dafalias, 1997), ISA defines a yield surface in the intergranular strain space - a state variable inspired by Niemunis and Herle (1997) that captures recent strain history. The model ensures stress rate continuity and transitions to a structure resembling hypoplastic models under larger strain amplitudes. ISA has since been extended to clays and coupled with other advanced models (e.g., barodesy, clay hypoplasticity) to improve predictions under cyclic loading.

The model introduces anisotropy via a back intergranular strain tensor and includes a fabric dilatancy tensor z. It shares conceptual similarities with the SANISAND model proposed by Manzari & Dafalias (2004) but differs in that it does not introduce a yield surface for the prediction of the overall mechanical behaviour.

ISA requires the calibration of 11 parameters (Knittel et al., 2023), including critical state parameters and characteristic void ratios, with four additional parameters for cyclic loading. Calibration was performed using the numgeo-ACT tool (Machacek et al., 2022) and the numgeo finite element code, based on 27 experimental tests summarized in Reid (2022). Differential Evolution optimization achieved good agreement for both drained and undrained tests. Table 2 summarizes the ISA parameters used in this study for the different sample preparation methods AD and MT, respectively.

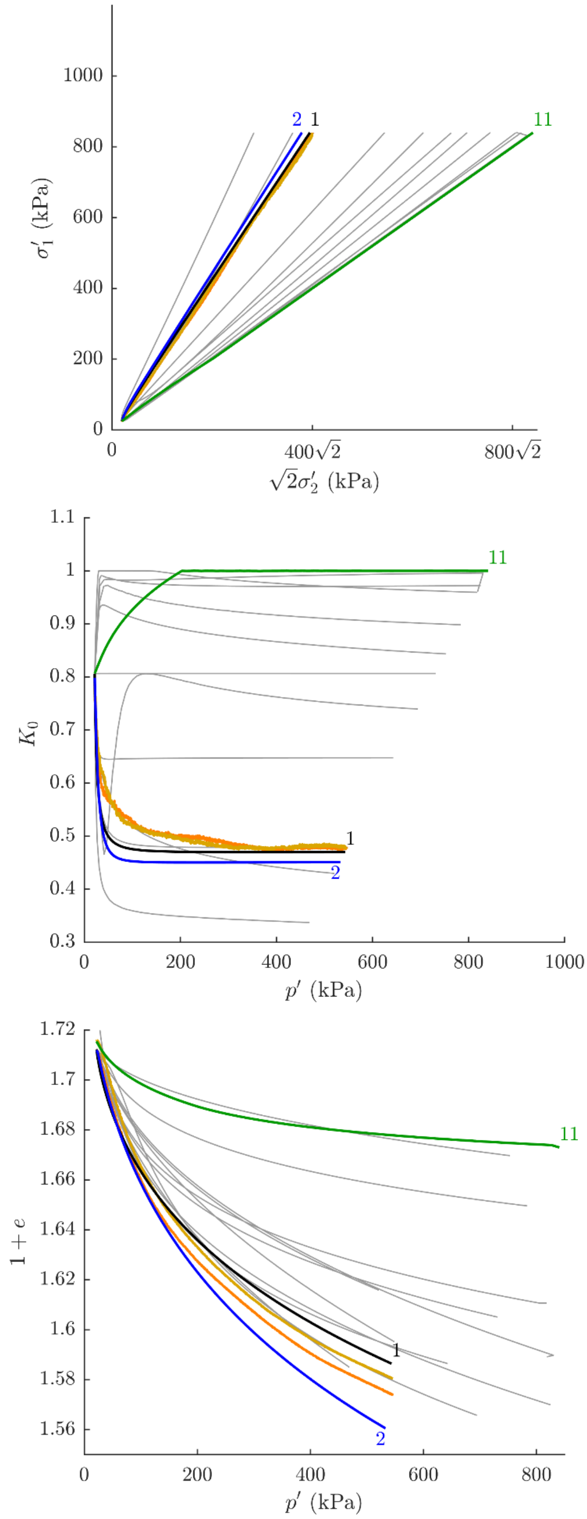

Figure 1. Oedometric compression: black: hypoplasticity, blue: ISA model, green: NorSand; orange lines show experimental results for the AD-prepared sample. Grey lines indicate predictions from other models. Figure modified from Reid et al. (2026).

Table 2. Parameters of ISA model for the MT and AD prepared samples (Group 2).

	λ_i	n_{pi}	n_{ei}	λ_c	n_{pc}
MT	0.01	0.439	3.579	0.0146	0.679
AD		0.5	2.636	0.0067	0.5

	e_{c0}	ν	M_c	n_d	f_{b0}
MT	0.7733	0.26	1.38	0.08	1.5
AD	0.7194	0.231	1.43		

	r_f	m_R	R	β	χ
MT	0.4	2.5	0.0001	0.2	2.0
AD	0.5				

2.3 *NorSand*

The NorSand model, introduced by Jefferies (1993), is a critical state-based elastoplastic constitutive framework developed for simulating the mechanical behaviour of granular materials such as sand and silt. It employs a bullet-shaped yield surface and aims to capture the dilatant behaviour of these materials using an associated plastic flow rule. A key feature of the model is the use of a state parameter, defined as the difference between the current void ratio and the void ratio at the critical state at the same mean effective stress. Similar to the original Cam-Clay formulation, the bullet-shaped yield surface leads to the unrealistic prediction of non-zero deviatoric plastic strain at zero deviatoric stress ($q = 0$); a modelling artefact that becomes particularly relevant when interpreting oedometer responses. Despite such limitations, the NorSand model has gained traction in practice, largely due to its implementation in several commercial software packages and its widespread adoption in geotechnical and mining applications. Calibrated parameters of the NorSand model are given in Table 3. However, we observed that the calibration tests did not yield a unique set of model parameters. In particular, multiple combinations of the parameters X_{tc}, H, and I_r were able to reproduce the calibration results with comparable accuracy.

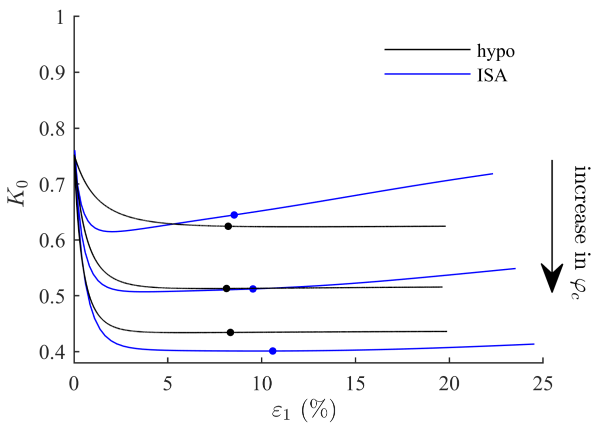

Figure 2. Simulations of oedometric compression tests with initial conditions according to Fig. 1 with φ_c = 20°, 30°, and 40°. In the ISA model, no constant K_0 value is reached within the investigated stress range, whereas the hypoplastic model approaches a constant K_0 value. Simulations were performed up to σ_1' = 10000 kPa, points indicate where σ_1' = 1000 kPa.

Table 3. Parameters of NorSand for the MT and AD prepared samples (Group 11).

M_{tc}	N	H	I_r	λ	ν	χ_{tc}	Γ
1.4	0.38	125	400	0.04	0.25	4	0.83

3 MODEL PREDICTIONS

This section presents model predictions for oedometric and hollow cylinder torsional shear tests, with a focus on comparing hypoplasticity, ISA model, and NorSand against experimental results. In addition to individual comparisons, we aim to give a broader view of consolidation paths for various deviatoric directions.

3.1 *Oedometric compression*

Figure 1 shows the model predictions for oedometric compression of the AD-prepared samples, compared with experimental results. The predicted curves from hypoplasticity (1), the ISA model (2), and NorSand (11) are shown alongside experimental data (orange) and predictions from other round-robin models (grey, Reid et al., 2026). The figure includes a σ_1'-$\sqrt{2}\,\sigma_2$' plot, a corresponding K_0- p' plot to capture the stress path evolution, and a *(1+e)-p'* plot for the volumetric response. The predictions of hypoplasticity and the ISA model capture both the stress path and the volumetric response well. In contrast, NorSand overpredicts the K_0 value and the stiffness in the volumetric response.

Applying a proportional strain path - a path with constant ratios of principal strain rates (as in oedometric compression) - leads to a stress path that approaches a constant stress ratio q/p', a so-called proportional stress path (Goldscheider, 1967; Chu & Lo, 1994).

This behaviour is a common feature of hypoplastic models (Gudehus & Mašín, 2009; Mašín, 2013; Mugele et al., 2024). From Figure 1, it appears that a constant K_0 value is reached for all models, but for higher stresses and when φ_c is varied, a different picture emerges for the ISA model. Figure 2 shows simulations with hypoplasticity and the ISA model of oedometric compression tests with initial conditions according to Figure 1 and critical friction angles φ_c = 20°, 30°, and 40°. Simulations were run up to σ_1' = 10000 kPa, the points indicate where σ_1' equals 1000 kPa. In the ISA model (using AD parameters from Table 2), a constant K_0 value was not reached within the investigated stress range, whereas the hypoplastic model reaches a constant K_0 value.

The higher the critical friction angle φ_c of a material, the lower the K_0 value. This trend is summarised in Figure 3, which compares the simulation results with Jáky's relation ($K_0 = 1 - \sin\varphi_c$), experimental data from Muir Wood (1990), and results from NorSand, the ISA model, hypoplasticity, and in red round-robin experimental data (Reid et al., 2026). For the ISA model, the K_0 values at σ_1' = 1000 kPa are plotted. ISA and hypoplasticity capture the dependence of K_0 on φ_c and remain close to Jáky's relation and the experimental range. In contrast, the values of K_0 predicted by NorSand remains close to 1, corresponding to a hydrostatic stress condition. To our understanding, this behaviour stems from the bullet-shaped yield surface adopted in NorSand, which permits non-zero deviatoric plastic strain rates even when the deviatoric stress $q = 0$. Such predictions are inherently excluded by yield surfaces with proper convexity at $q = 0$, such as the elliptical surface used in the Modified Cam-Clay model, which does not allow for deviatoric plastic flow under hydrostatic loading. The lower accuracy of the NorSand model is partly due to the non-unique calibration, as mentioned earlier. It is indeed possible, in retrospect, to recalibrate the NorSand parameters to better match K_0 values inferred from oedometer tests. However, the core issue pertaining to the deviatoric plastic flow under hydrostatic stress appears to be a fundamental limitation of the yield surface formulation, rather than a calibration artefact.

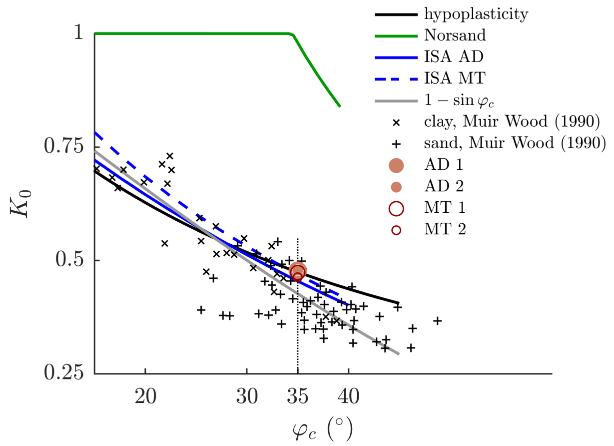

Figure 3. Comparison of K_0 *vs.* φ_c relation: Jáky's relation, experimental data (Muir Wood, 1990), model predictions, and round-robin experimental results (Reid et al., 2026).

3.2 *Hollow cylinder torsional shear tests*

In the hollow cylinder torsional shear (HCTS) tests, plane-strain direct simple shear (DSS) consolidation was prescribed along linear σ'-τ paths, leading to specified final values of vertical stress σ' and shear stress τ. From these tests, the Lode angle Θ, the angle of stress rotation α, and thus the principal stress state was determined. In addition, the volumetric response was obtained. In this study, the angle of principal stress rotation α is defined as the angle between the major principal stress direction and the vertical axis. The Lode angle defines the deviatoric direction of a stress state; Θ = +30° corresponds to axisymmetric triaxial compression, and –30° to axisymmetric triaxial extension.

3.2.1 *Predictions from the round robin*

For the HCTS predictions using hypoplasticity and ISA, the final values of α for the AD sample in Figure 4 are 23.4° and 23.0°, respectively. According to hypoplasticity, the Lode angle at final state is $\Theta = 21.5°$, for ISA it is $\Theta = 21.9°$. The predictions of hypoplasticity and the ISA models indicate close agreement with the experimental results in terms of angle of stress rotation α and the Lode angle Θ, whereas NorSand overpredicts α and underpredicts Θ. Both, α and Θ then define the principal stress state and thus p'. The stress path in the p'-q plane is approximately linear, located between the hydrostatic axis and the critical state line, similar to oedometric compression. Hypoplasticity and ISA capture this p'-q evolution well, whereas NorSand underpredicts the stress ratio q/p'.

3.2.2 *Investigations in the deviatoric plane*

To obtain a broader view of the stress paths resulting from different proportional strain paths, we apply strain paths with constant contractancy $\delta = \mathrm{tr}(\boldsymbol{\varepsilon})/|\boldsymbol{\varepsilon}|$, defined based on the total strain rate, in various deviatoric directions. Oedometric compression follows a strain path with constant contractancy (δ = 1, with positive strain rate in compression). The HCTS tests follow such a path with $\delta \approx 0.77$ (see Figure 5). Isochoric strain paths (δ = 0) lead to critical stress states, while oedometric compression ($\delta = 1$) approaches the K_0 stress path. Proportional strain paths with $\delta = 0$, 0.77, and 1 are applied in various deviatoric directions. In hypoplasticity, isochoric strain paths (δ = 0) approach the Matsuoka–Nakai critical stress surface (Matsuoka and Nakai, 1985), while in the ISA model, they approach the surface proposed by Argyris et al. (1974), see Figure 6. Strain paths with $\mathrm{tr}(\boldsymbol{\varepsilon})/|\boldsymbol{\varepsilon}| = 1$ form a cone in principal stress space that includes the oedometric K_0 state under axisymmetric conditions (Figure 6). An intermediate value, such as $\delta = 0.77$ from the HCTS tests, produces a cone located between the other two.

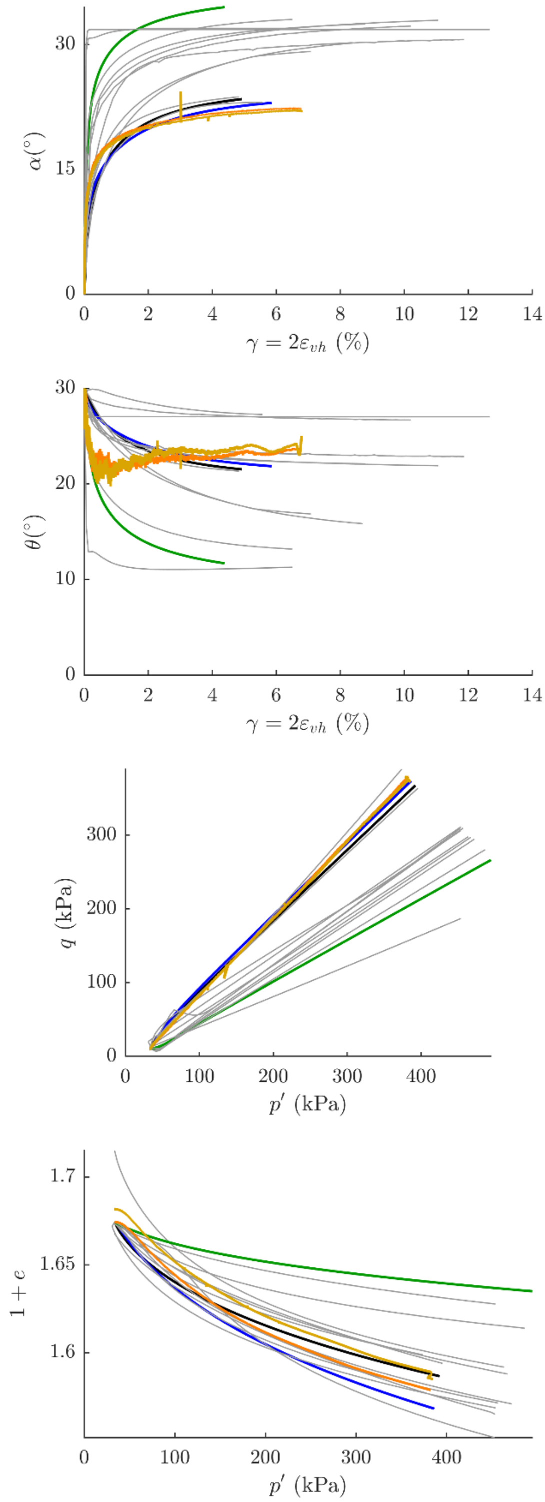

Figure 4. HCTS AD (orange); black: hypoplasticity, blue: ISA model, green: NorSand; Figure modified from Reid et al. (2026).

Thin lines represent predictions from hypoplasticity; thick lines show results from the ISA model. The stress paths of the HCTS experiments (in grey) end near the cones generated with $\delta = 0.77$. The two deviatoric directions tested in the experiments (Θ=30° and Θ~21.5° for the HCTS), combined with three different dilatancies, provide experimental points that lie close to the cones predicted with hypoplasticity and ISA; the results from MT and AD prepared samples fall close to each other. Figure 7 shows the corresponding lines in the p'-q plane, based on the results from Figures 5 and 6.

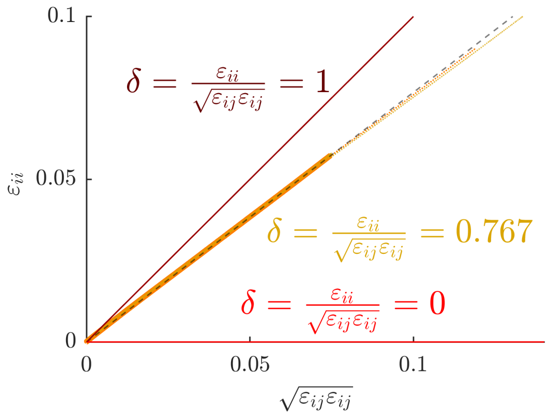

Figure 5. δ=tr($\boldsymbol{\varepsilon}$)/|$\boldsymbol{\varepsilon}$| = 1 applies for oedometric compression, δ=tr($\boldsymbol{\varepsilon}$)/|$\boldsymbol{\varepsilon}$| ~ 0.767 ~ constant in all HCTS tests; AD (orange solid lines), MT (orange dotted lines), and strain paths with δ=tr($\boldsymbol{\varepsilon}$)/|$\boldsymbol{\varepsilon}$| = 0 will lead to critical stress states.

As shown in Figure 2, hypoplasticity approaches proportional stress paths, while the ISA model does not within the investigated stress range of less than 10000 kPa. For the ISA model, simulations with $\delta = 0.77$ and 1 were therefore run from $p' = 1$ kPa up to 1000 kPa, starting from a loose state. Final stress states were plotted to visualise the resulting surfaces. Only in the isochoric case ($\delta = 0$), the stress paths reach a constant q/p' value, corresponding to the Argyris surface.

4 DISCUSSION

The round-robin benchmarking exercise provides insights into why constitutive models differ under varying initial conditions and loading paths. In the following, we discuss aspects related to model calibration and the influence of sample preparation.

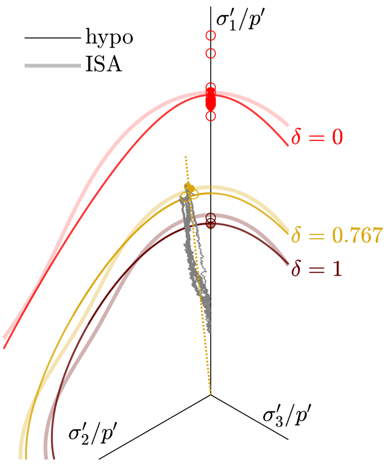

Figure 6. Applying proportional strain paths with constant dilatancies according to Figure 5 in different deviatoric directions leads to different cones, here shown in normalized deviatoric plane; cones obtained from simulations with hypoplasticity and the ISA model, the orange dotted line indicates a Lode angle of 21.5°; experimental results from Reid et al. (2026) are added, AD: bullets, MT: circles, the HCTS experimental path are added in grey.

4.1 *Model calibration under varying initial conditions – on the role of parameters versus sample preparation effects*

Group 1 and 11 used the same parameter set for both AD and MT samples to emphasise that model parameters are intended to describe the soil type, not the sample preparation method (see Tables 1, 2 and 3). In contrast, Group 2 applied different parameter sets for AD and MT samples, acknowledging that the spreparation method affects the soil fabric and thus the mechanical response. In the absence of explicit state variables to describe fabric effects, this influence was captured by calibrating separate parameter sets.

The results show that even with a single set, model trends match experimental behaviour. If the samples are consolidated, the MT tests generally result in higher void ratios than AD tests. Groups 1 and 11 therefore accounted for the effect of sample preparation through the initial void ratio, which is a state variable in all three models. For more substantial structural changes, an additional state variable - such as the one introduced by Mašín (2007) - would be required. However, due to hypoplasticity's ability to predict trends of MT and AD prepared samples well, the standard formulation was retained without an explicit structure variable.

4.2 *Calibration based on standard tests*

Calibration should be based on standard laboratory tests (isotropic/oedometric compression tests, CD/CU tests) as proposed, for example, by Herle (1997). Model developers are responsible for validating robustness under conditions more general loading paths, stress rotation, and varying Lode angles, so that users can rely on simple calibration procedures. However, such validations are not always available, which motivated the present study.

5 CONCLUSIONS

This study evaluated three constitutive models - hypoplasticity, ISA, and NorSand - based on blind predictions of oedometric and hollow cylinder torsional shear tests in a round-robin exercise. Hypoplasticity and the ISA model showed good agreement with experimental results across different loading conditions, while NorSand exhibited limitations. Key factors contributing to the performance of the models include consistent calibration and the models' ability to handle stress rotation and non-axisymmetric conditions. Reliable application in practice requires well-defined calibration based on standard tests, supported by broader model validation: in addition to comparing individual experiments, this study also demonstrates more general validation approaches - such as the K_0 vs. φ_c relation and representations in the deviatoric plane - which are important to assess a model's generality beyond a few selected experiments.

6 ACKNOWLEDGEMENTS

This research was funded in part by the Austrian Science Fund (FWF) 10.55776/V918. G.M. is funded by the FWF. For open access purposes, the author has applied a CC BY public copyright license to any author accepted manuscript version arising from this submission.

7 DATA AVAILABILITY STATEMENT

The experimental data used for model calibration are available in *Reid (2022)*: doi: 10.17605/OSF.IO/RTJ3P

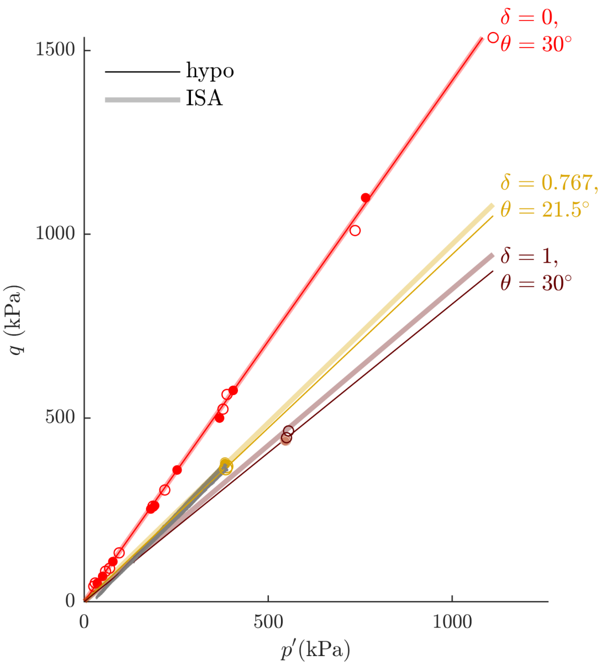

Figure 7. p'-q plot corresponding to Figure 6. The orange line indicates q/p' along the δ=tr($\boldsymbol{\varepsilon}$)/|$\boldsymbol{\varepsilon}$| = 0.767 cone obtained with hypoplasticity (thin line) and ISA (thick line) at a Lode angle of 21.5°; the dark red line is the K_0 path of hypoplasticity (thin line) and ISA (thick line); the red line is the CSL for axisymmetric conditions. Experimental results (Reid et al., 2026) are added: bullets: AD samples, circles: MT samples; the HCTS experimental stress paths, shown in grey and lying approximately within the stress range p'=30-380 kPa overlap with the predictions of hypoplasticity and ISA for δ = 0.767.

8 REFERENCES

Argyris, J.H., Faust, G., Szimmat, J., Warnke, E.P., and Willam, K.J. (1974). Recent developments in the finite element analysis of prestressed concrete reactor vessels. *Nuclear Engineering and Design*, 28(1), 42–75.

Bauer, E., 1996. Calibration of a comprehensive hypoplastic model for granular materials. *Soils and Foundations*, 36(1), pp.13–26.

Chu, J. and Lo, S.-C.R. (1994). *Asymptotic behaviour of a granular soil in strain path testing*. Géotechnique, 44(1), 65–82.

Fuentes, W., and Triantafyllidis, T. (2015). ISA model: a constitutive model for soils with yield surface in the intergranular strain space. *International Journal for Numerical and Analytical Methods in Geomechanics*, 39(11), pp. 1235-1254.

Gudehus, G. and Mašín, D., 2009. Graphical representation of constitutive equations. *Géotechnique*, 59, pp.147–151.

Goldscheider, M. (1967). *Grenzbedingung und Fließregel von Sand*. Mechanics Research Communications, 3, 463–468.

Herle, I., 1997. *Hypoplastizität und Granulometrie einfacher Korngerüste*. PhD thesis. Veröffentlichungen des Institutes für Bodenmechanik und Felsmechanik der Universität Karlsruhe, No. 142.

Herle, I. and Gudehus, G., 1999. Determination of parameters of a hypoplastic constitutive model from properties of grain assemblies. *Mechanics of Cohesive-Frictional Materials*, 4(5), pp.461–486.

Jefferies, M.G., 1993. Nor-Sand: a simple critical state model for sand. Géotechnique, 43(1), pp.91-103.

Kadlíček, T., Janda, T., Šejnoha, M., Mašín, D., Najser, J. and Beneš, Š., 2022. Automated calibration of advanced soil constitutive models. Part I: hypoplastic sand. *Acta Geotechnica*, 17, pp.3421–3438.

Knittel, L., Tafili, M., Tavera, C. G., and Triantafyllidis, T. (2023). New perspectives on preshearing history in granular soils. *Scientific Reports*, 13(1), pp. 4576.

Machaček, J., Staubach, P., Tavera, C. E. G., Wichtmann, T., and Zachert, H. (2022). On the automatic parameter calibration of a hypoplastic soil model. *Acta Geotechnica*, 17(11), 5253-5273.

ssManzari, M. T., and Dafalias, Y. F. (1997). A critical state two-surface plasticity model for sands. *Géotechnique*, 47(2), 255-272.

Mašín, D., 2007. A hypoplastic constitutive model for clays with meta-stable structure. *Canadian Geotechnical Journal*, 44(3), pp.363–375.

Mašín, D., 2013. Clay hypoplasticity with explicitly defined asymptotic states. *Acta Geotechnica*, 8, pp.481–496.

Matsuoka, H. and Nakai, T. (1985). Relationship among deviator, principal stress, and failure surface in three-dimensional stress space. *Soils and Foundations*, 25(3), 123–134.

Mugele, L., Stutz, H.H. and Mašín, D., 2024. Generalized intergranular strain concept and its application to hypoplastic models. *Computers and Geotechnics*, 173, 106480.

Muir Wood, D., 1990. *Soil behaviour and critical state soil mechanics*. Cambridge: Cambridge University Press.

Niemunis, A., and Herle, I. (1997). Hypoplastic model for cohesionless soils with elastic strain range. *Mechanics of Cohesive-frictional Materials*, 2(4), 279-299.

Reid, D., Fanni, R., Fourie, A., Medicus, G., Mašín, D., Tafili, M., Staubach, P., Han, C., Ludlow, W., Taiebat, M., Zheng, S., Cheng, Z., Chen, V., Wang, Y., Pinedo, P., Monforte, L., Zhou, H., Ragni, R., Singh, V., Simms, P., Mofrad, M., Pouragha, M., Fayek, S., Ayawah, P., Brink, N., Greyling, D., Gidley, I., Irandoost, E., Coyle, E., & James, A., Ndlovu, I. (2026). *Blind constitutive model predictions of below-slope stress conditions: A round-robin study*. preprint: doi: 10.17605/OSF.IO/SDKFX

Reid, D. (2022). *Slope stress prediction benchmarking exercise: Triaxial calibration data*. [online] doi: 10.17605/OSF.IO/RTJ3P [Accessed: 10 June 2025]

von Wolffersdorff, P.-A. (1996) A hypoplastic relation for granular materials with a predefined limit state surface. *Mechanics of Cohesive-Frictional Materials* 1(3): 251–271.